



Loss of intestinal nuclei and intestinal integrity in aging *C. elegans*

Matthew D. McGee,¹ Darren Weber,¹ Nicholas Day,¹ Cathy Vitelli,¹ Danielle Crippen,¹ Laura A. Herndon,² David H. Hall² and Simon Melov¹

¹Buck Institute for Age Research, 8001 Redwood Blvd, Novato, CA 94945, USA

²Albert Einstein College of Medicine, Center for *C. elegans* Anatomy, 1410 Pelham Parkway South, Rm 601, Bronx, NY 10461, USA

Summary

The roundworm *C. elegans* is widely used as an aging model, with hundreds of genes identified that modulate aging (Kaeberlein *et al.*, 2002. *Mech. Ageing Dev.* 123, 1115–1119). The development and bodyplan of the 959 cells comprising the adult have been well described and established for more than 25 years (Sulston & Horvitz, 1977. *Dev. Biol.* 56, 110–156; Sulston *et al.*, 1983. *Dev. Biol.* 100, 64–119). However, morphological changes with age in this optically transparent animal are less well understood, with only a handful of studies investigating the pathobiology of aging. Age-related changes in muscle (Herndon *et al.*, 2002. *Nature* 419, 808–814), neurons (Herndon *et al.*, 2002), intestine and yolk granules (Garigan *et al.*, 2002. *Genetics* 161, 1101–1112; Herndon *et al.*, 2002), nuclear architecture (Haithcock *et al.*, 2005. *Proc. Natl Acad. Sci. USA* 102, 16690–16695), tail nuclei (Golden *et al.*, 2007. *Aging Cell* 6, 179–188), and the germline (Golden *et al.*, 2007) have been observed via a variety of traditional relatively low-throughput methods. We report here a number of novel approaches to study the pathobiology of aging *C. elegans*. We combined histological staining of serial-sectioned tissues, transmission electron microscopy, and confocal microscopy with 3D volumetric reconstructions and characterized age-related morphological changes in multiple wild-type individuals at different ages. This enabled us to identify several novel pathologies with age in the *C. elegans* intestine, including the loss of critical nuclei, the degradation of intestinal microvilli, changes in the size, shape, and cytoplasmic contents of the intestine, and altered morphologies caused by ingested bacteria. The three-dimensional mod-

els we have created of tissues and cellular components from multiple individuals of different ages represent a unique resource to demonstrate global heterogeneity of a multicellular organism.

Key words: *C. elegans*; nucleus; aging; intestine; microvilli.

Introduction

Several important studies have described morphological changes with age in the nematode *C. elegans*. These include specific changes in tissues such as the muscle (Herndon *et al.*, 2002), gonad (Garigan *et al.*, 2002; Golden *et al.*, 2007), pharynx (Garigan *et al.*, 2002), and hypodermis (Golden *et al.*, 2007) as well as some changes at the subcellular level (Haithcock *et al.*, 2005). This handful of studies represent the state of our knowledge regarding the pathological changes that arise with age in *C. elegans*. Despite over 20 years of investigation using *C. elegans* as a model system to better understand the interplay between gene action and longevity (Johnson, 2002), we remain remarkably ignorant about how aging affects (or does not affect) cell function or morphology for each of the 959 cells comprising the adult nematode.

There are three major epithelial tissues in *C. elegans*: the pharynx, intestine, and hypodermis. Of these three, the intestine is the least characterized in aging *C. elegans*. During development, the two intestinal primordial cells gastrulate, divide, polarize, and intercalate, forming an intestine composed of 20–21 cells at hatching. Two of these intestinal cells, bound tightly by an adherens junction, border the lumen in any one region of the intestine. The microvilli, which contain a core of actin filaments that are anchored by the terminal web of intermediate filaments, protrude from the apical membranes of these cells. Some of the intestinal nuclei divide and become binucleate, resulting in a total of 30–34 intestinal nuclei. These nuclei endoreduplicate during each larval molt, producing 32C per nucleus by adulthood and resulting in visibly larger nuclei (Sulston & Horvitz, 1977; Hedgecock & White, 1985; Leung *et al.*, 1999; Hall & Altun, 2008). Although the development of the intestine has been very well described through the young adult stage (3 days of age), the aging pathology of this tissue has not. Previous descriptions of age-related intestinal changes were limited to qualitative observations of accumulated bacteria in the intestine (Garigan *et al.*, 2002) and an accumulation of intestinally produced yolk in the body cavity (Garigan *et al.*, 2002; Herndon *et al.*, 2002).

Loss of specific cell types with increasing chronological age can be a characteristic pathological hallmark of tissues in aging mammals. For example, more than 50% of men over the age of

Correspondence

Simon Melov, Buck Institute for Age Research, 8001 Redwood Blvd, Novato, CA 94945. Tel.: 415-209-2000; fax: 415-899-1810; e-mail: smelov@buckinstitute.org

Accepted for publication 12 March 2011

80 have some degree of functional muscle loss (sarcopenia) that is clinically significant (Thomas, 2010). *C. elegans* has a tremendous potential for quantifying the loss of specific cells or nuclei with age, owing to its optical transparency, and completely defined cell lineage. Accordingly, we set out to integrate a suite of techniques that could be applied to better understand the fate of specific defined nuclei within the aging nematode. Here, we describe for the first time in detail the aging pathology of the *C. elegans* intestine. Our novel approach confirmed previous observations of bacterial and yolk accumulation in the aging intestine. We also report major age-related changes that were regionally specific, progressive degradation and sometimes complete loss of intestinal microvilli, major degradation and loss of intestinal nuclei, and changes in the size, shape, and cytoplasmic contents of the intestine. We took a unique approach to investigate aging pathology by combining three complementary methods: traditional histological staining of sectioned tissues, transmission electron microscopy, and confocal fluorescence microscopy combined with 3D volumetric reconstruction. This

synergistic approach of combining computationally intensive 3D modeling with traditional morphological techniques allowed us to reconstruct tissues, proteins, and organelles in three dimensions in the whole worm at different ages. This afforded us an unprecedented visualization of aging at the whole organism level at high resolution, which will facilitate additional studies in other tissues, allowing us to quantify and better understand which cells are vulnerable to the degenerative changes in age.

Results

Age-related intestinal phenotypes

We utilized both light and transmission electron microscopy to determine the fate of various tissues relating to the aging *C. elegans* intestine. We observed massive changes in the organization and structure of this tissue. First, we embedded young and old wild-type (N2) hermaphrodite whole worms in plastic. Entire animals were sectioned at a thickness of 0.5 μm (resulting

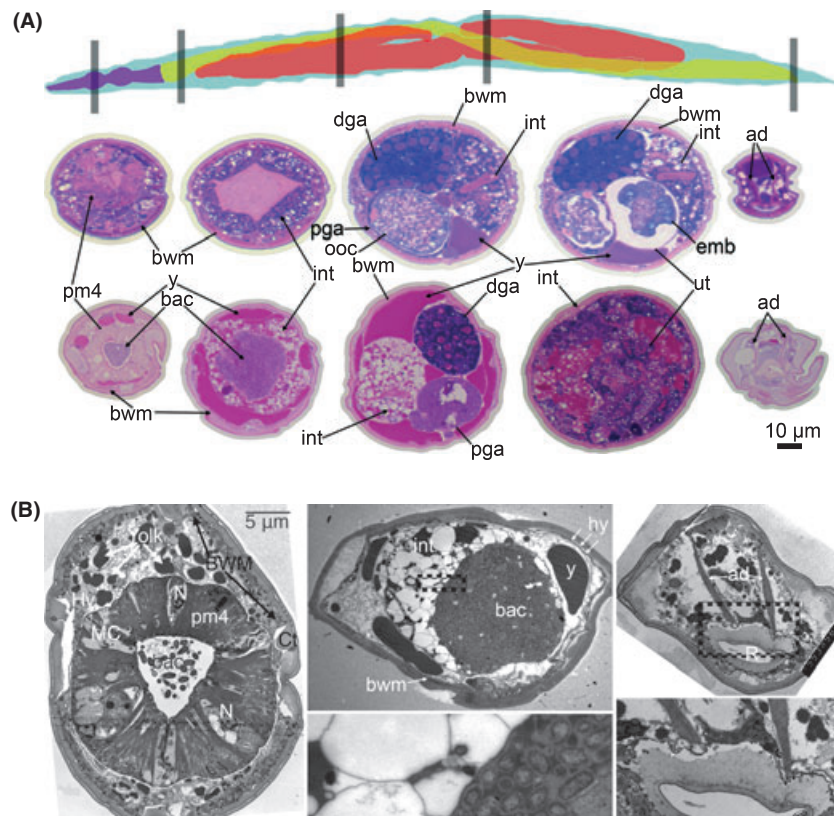


Fig. 1 Pathobiology of aging *C. elegans* tissues. (A) Tissue sections stained with pararosaniline and methylene blue from equivalent regions of a 4-day-old and 20-day-old wild-type worm. Shown in the top is a schematic of the lateral view of a wild-type worm showing pharynx (purple), intestine (yellow), and gonad (red). The regions shown in the bottom sections are represented by gray boxes. The middle row is the 4-day-old worm, and the bottom row is the 20-day-old worm. Left to right, the regions are the head containing the pharynx, the region immediately posterior to the pharynx, the midbody containing the distal and proximal gonad arms, the midbody containing the uterus, and the rectum. Body wall muscle (bwm), intestine (int), distal gonad arm (dga), proximal gonad arm (pga), oocytes (ooc), embryos (emb), uterus (ut), anal dilator (ad), pharyngeal muscle (pm4), bacteria (bac), and yolk particles (y) are labeled. The intestine is barely visible as a thin pink wedge in the fourth section from the 20-day-old worm. Scale bar is 10 μm . (B) Representative transmission electron micrographs from 18-day-old wild-type worms showing the pharynx, the region immediately posterior to the pharynx, and the rectum. Zoomed regions below their respective images are indicated by dotted lines of the bacterial packing in the intestine and the rectum. The intestinal lumen in a class 'C' animal shows no microvilli facing the clustered bacteria, and the intestinal cytoplasm is dominated by empty vacuoles and a lack of ground substance. Other organelles are profoundly diminished. Pharynx and rectum TEMs come from class 'B' animals.

in approximately 2000 serial sections per worm), and the cross-sections stained with the histological stains methylene blue and pararosaniline (Figs 1A, 3C and S1, Movies S1 and S2). Methylene blue primarily stains DNA, and pararosaniline is a general histological stain that labels many tissue types (Gomori, 1950). Transmission electron microscopy of similarly aged worms allowed higher resolution of small structures (Figs 1B, 2, 4, 7 and S2).

The intestine is first reshaped during late larval development when the expanding reproductive system pushes the intestine to the side of the body cavity (Sulston & Horvitz, 1977; Kimble & Hirsh 1979; Hall & Altun, 2008). During the later stages of aging, the germline progressively swells (Golden *et al.*, 2007), pressing against the intestine enough to cause severe thinning of the intestinal epithelium, particularly along the midbody (Figs 1 and S1). During larval development and early adulthood, the intestinal cells have enough structural integrity to be reshaped without damage, but intestinal cells weaken during aging until this continued germline pressure causes dramatic distortions of the intestine and its lumen, possibly leading to the blockage of luminal flow and bacterial buildup (Fig. 3, Movie S3).

Consistent with other reports (Garigan *et al.*, 2002), we found large pockets of undigested bacteria that were often visible in the intestinal lumen. This appears as dark purple stain in methylene blue/pararosaniline-stained sections (Figs 1A and S1, Movies S1 and S2). By using all the sections from a whole worm, we are able to observe in detail where the pockets of undigested bacteria are localized (Movie S1). These bacteria are most common near the pharynx, with many regions of the middle and posterior intestinal lumen completely empty (Figs 1 and S1). Intact bacteria are clearly visible in transmission electron micrographs, in both the pharyngeal lumen and intestinal lumen (Figs 1B, 4 and S2). These bacteria are likely undigested because of reduced pharyngeal pumping and poor grinder function (Collins *et al.*, 2008). As they accumulate inside the lumen, these intact bacteria can undergo cell divisions and swell the lumen dramatically. In some cases, intact bacteria were also observed to invade the lumen of the uterus and spermatheca (entering via the vulva), or to cross into cells along the alimentary canal, passing through the luminal plasma membrane and into the marginal cells of the pharynx (Fig. 2). Similar bacterial infections are known to occur in some nematode species as an adaptive mechanism with a commensal bacterial species or sometimes as a toxic invasion (Ciche *et al.*, 2008; Irazoqui *et al.*, 2010). While we generally view *E. coli* as a nutritious nematode 'food', and standard laboratory conditions saturate the animal in food, in extreme aging, the nematode may be overcome and killed by *E. coli* infection. In some portions of the intestinal lumen, bacteria appear to undergo a change in state and become actively damaging to the microvilli (Fig. 4I–N).

Like others (Garigan *et al.*, 2002; Herndon *et al.*, 2002), we also observed changes in yolk particles with age. Yolk particles are normally synthesized in the intestine and secreted into the body cavity (the pseudocoelom), where they travel to the germline (Kimble & Sharrock, 1983; Hall *et al.*, 1999). Methylene

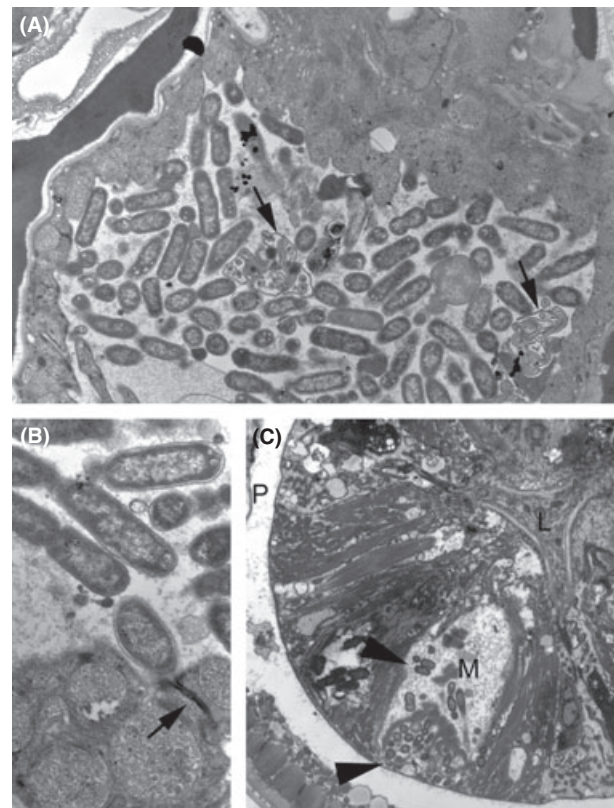


Fig. 2 Bacteria invade old worms. (A) Eighteen-day-old class 'B' adult. Live bacteria are clustered inside the spermathecal lumen. Arrows indicate several spermatocyte remnants lying among the bacteria. These bacteria have probably entered via the open vulva and become concentrated here at the distal end of the uterus, where immature oocytes likely block them from further migration into the gonad arm. (B) Closeup of same animal shows healthy bacteria at higher power. Arrow indicates an adherens junction between two epithelial cells, blocking the bacteria from crossing the epithelium and into the body cavity. (C) Eighteen-day-old class 'A' animal. Live bacteria (arrowheads) are clustered inside the marginal cell (M) of the pharynx, particularly near the basal zone near the body cavity, or pseudocoelom (P), although smaller clusters lie throughout the marginal cell. It is not certain whether these bacteria have penetrated into the cell via the basal pole, in which case they may have originally crossed through the intestine to reach the pseudocoelom, or whether they crossed the apical membrane from the pharyngeal lumen (L). As there was no evidence of free bacteria in the body cavity by TEM in this animal, we suspect that entry was via the apical pole.

blue/pararosaniline staining and transmission electron micrographs show yolk particles (Garigan *et al.*, 2002; Herndon *et al.*, 2002) accumulating in the body cavity of old individuals (Figs 1, 4 and S1, Movies S1 and S2). These yolk particles appear as magenta in methylene blue/pararosaniline-stained sections (Figs 1A and S1, Movies S1 and S2). Prior reports have described age-related yolk accumulation using different techniques (Garigan *et al.*, 2002; Herndon *et al.*, 2002). The effects of this yolk accumulation are not currently known, but we hypothesize that the accumulation is caused by the age-related changes in the intestine and germline (Golden *et al.*, 2007), as these tissues are the site of yolk synthesis and the principal deposition site of yolk, respectively. We report here age-related changes in the intestine, which we hypothesize could cause an overproduction of

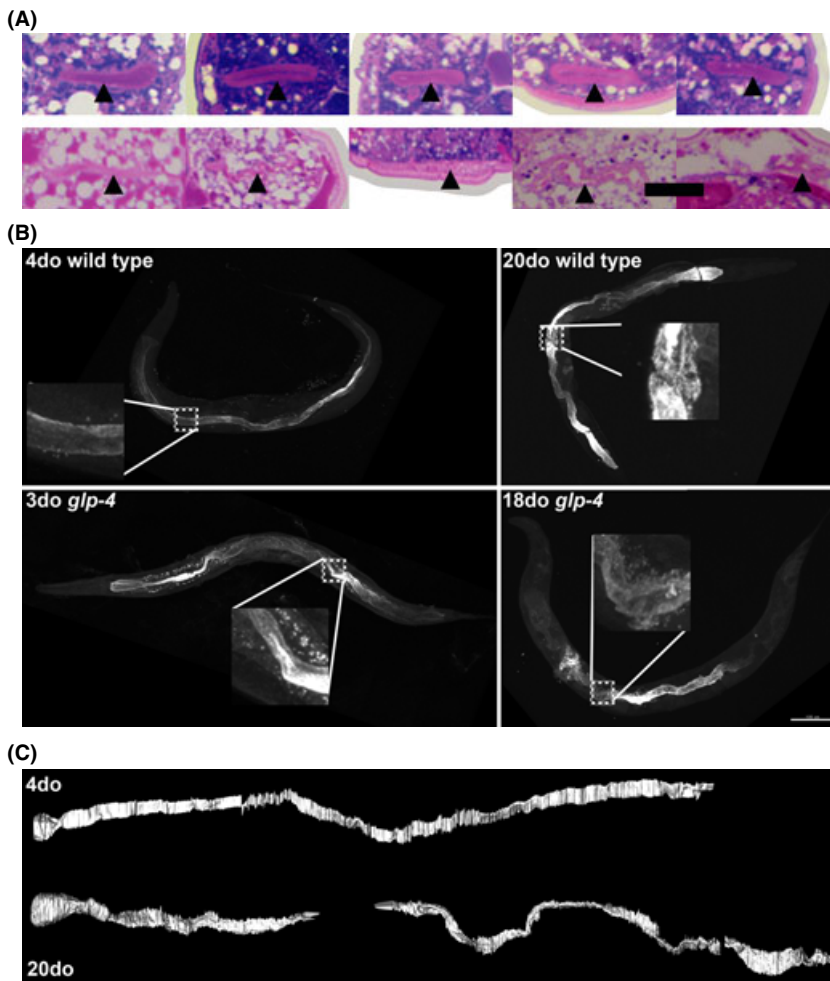


Fig. 3 Intestinal lumen becomes irregular and angular with age. (A) Five images of the intestinal lumen of a single 4-day-old (top row) and 20-day-old (bottom row) wild-type worm. Images are spaced 200 μm apart, starting after the anterior gonad arm. Scale bar is 10 μm . (B) Indirect immunofluorescence using an antibody specific to the intestinal lumen (MH33) from young (4-day-old) and old (20-day-old) wild-type worms and young (3-day-old) and old (18-day-old) *glp-4* worms. Insets are enlarged from boxed regions. Intestinal lumen is compressed, but not discontinuous, in the region containing germline swelling in the 20-day-old wild-type worm inset. Scale bar is 100 μm . (C) Segmentation of intestinal lumen from a young and old wild-type worm from aligned methylene blue/pararosaniline-stained tissue sections. Aging lumen is more highly kinked and seemingly discontinuous in places. These regions likely are not discontinuous, but merely compressed from germline swelling.

yolk. We find that the germline is also affected by aging in a manner that may limit yolk absorption (in preparation).

Other notable age-related changes in tissue morphology include body wall muscle degeneration, an accumulation of chromatin in over-proliferating germline cells (Golden *et al.*, 2007), and changes in intestinal morphology (Figs 1, 3 and S1, Movies S1 and S2). The body wall muscle degeneration has been well described elsewhere (Herndon *et al.*, 2002). Here, we focus on the age-related intestinal changes including changes in intestinal nuclei.

Age-related degradation of the intestinal lumen

We assayed changes in luminal structure by both immunofluorescence (Fig. 3B) and segmentation of aligned pararosaniline/methylene blue-stained sections (Fig. 3A,C). Except for a localized anterior swelling near the pharynx, the intestinal lumens of young animals are very uniform in their size and shape throughout the entire length of the intestine. Microvilli within the young adult intestine also appear to have a consistent anatomy from cell to cell, except for those within the first and last rings of cells, INT1 and INT9, where villi are foreshortened (Fig. S2). In contrast, old intestinal lumens appear thinner, tortu-

ous, and sometimes balloon locally (Fig. 3, Movie S3). To determine the shape of intestines, we segmented the intestinal lumen from aligned methylene blue/pararosaniline sections (Fig. 3C, Movie S3). The computer-generated surface model of the young intestine shows a relatively smooth structure that maintains an even thickness and size. The old intestine fluctuates dramatically in size and shape (Figs 3 and S1, Movie S3). In regions with swelling germline (Golden *et al.*, 2007), the intestine is compressed against the side of the worm (Fig. 3A, Movie S2), making the intestine difficult to resolve by pararosaniline/methylene blue staining. The age-related germline swelling can take up most of the volume of the worm and is usually confined to the uterus (Fig. S1, Movies S1 and S2). We will describe this in more detail in future publications. Sometimes this swelling causes an apparent gap in the intestinal lumen (Fig. 3C, Movie S3). However, the lumen can still be observed by immunofluorescence (Fig. 3B) and transmission electron microscopy (Fig. 4), suggesting that there is still a continuous structure. Breaks in the intestine are sometimes observed in old worms by fluorescence microscopy (Fig. 3B). However, we surmise these breaks occur during fixation as they would otherwise be immediately fatal. Therefore, there is unlikely to be any intestinal discontinuity, even in old individuals.

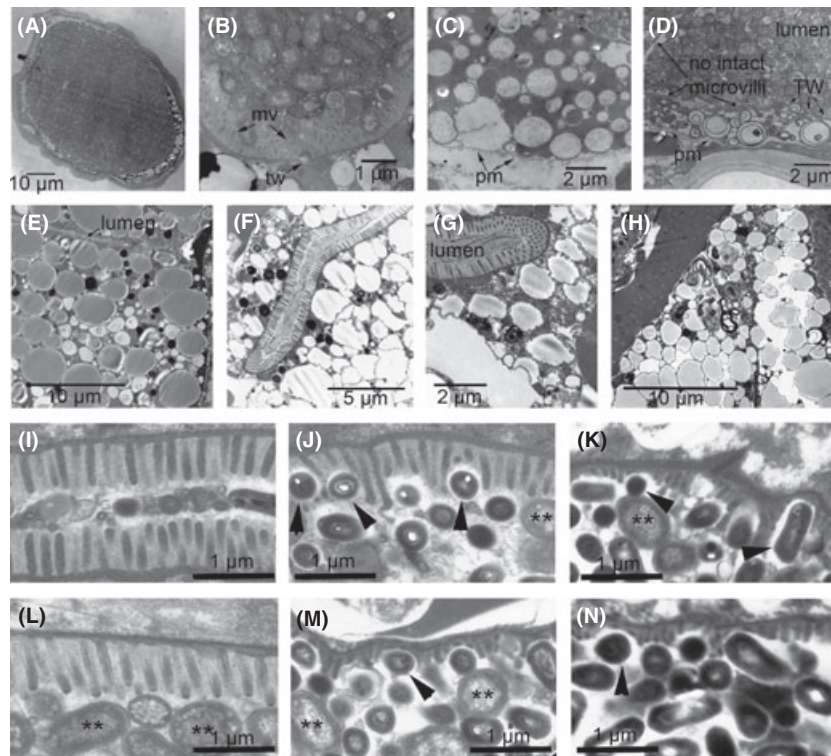


Fig. 4 Intestinal microvilli degrade and are lost with age. Representative transmission electron micrographs showing different regions of the intestine in 18-day-old (A–H) and 10-day-old (I–N) wild-type worms. Class ‘A’ (E), class ‘B’ (D, F–N), and class ‘C’ (A–C) animals are represented. Some regions in 18-day-old intestines completely lack microvilli (mv) projecting inward toward the lumen and instead display an unadorned plasma membrane (pm) (C, D). Even in the absence of microvilli, an intact terminal web (tw) may still protect the lumen from bacterial invasion into the cytoplasm of the intestine. Panels A–D show the lumen packed with bacteria. Panels E–H show regions where the lumen is empty, but cytoplasm is filled with large vesicles containing lipid or yolk, but shows little ground substance, ribosomes, or RER. Panels I–K come from three different intestinal cells in a 10-day-old adult. Panels L–N come from three different cells in another 10-day-old adult. Microvilli in I and L show a 50% shrinkage in length compared with young adult intestine, with all microvilli changing in length equally, either in the absence of bacteria (I) or in the presence of bacteria (J). A fuzzy glycocalyx seems to cover most ‘healthy’ microvilli (I, J, L) on their outer borders, protecting them from the luminal contents. In panels J, K, M, and N, smaller, dark-staining bacteria appear to insert themselves between villi and cause individual villi to become corroded, becoming both shorter and thinner. Double asterisks indicate intact OP50 *E. coli* in stasis. Black arrowheads indicate smaller bacteria that appear to cause corrosion of microvillar structures, where the glycocalyx may be reduced or absent.

As we observed significant changes in the overall structure of the intestinal lumen (Fig. 3), we tested whether there were changes in the microvilli. We compared animals of different movement classes, ‘A’ through ‘C’ (Hosono, 1978; Herndon *et al.*, 2002). Class ‘A’ animals have the most healthy movements, while class ‘C’ animals are relatively immobile (Hosono, 1978; Herndon *et al.*, 2002). We occasionally observed a complete loss of microvilli, which normally face the lumen, in some regions of old intestines from both class ‘B’ and class ‘C’ animals in transmission electron micrographs (Fig. 4, Table 1). Class ‘A’ animals did not have severe defects in their cytoplasmic contents, except for a large buildup in lipid storage (Table 1, Fig. 4E)(Herndon *et al.*, 2002). The integrity of the intestine as a whole is dependent on the plasma membrane, the presence of strong intercellular junctions linking adjacent intestinal cells, and a terminal web of actin microfilaments underlying the apical microvilli. As aging progresses, there is a weakening of the plasma membrane as evidenced by the microvilli changes (Fig. 4), but rarely is there any obvious weakening of the terminal web or cell junctions. The terminal web may be critical to the

Table 1 Intestine phenotypes (average microvilli shortening†)

Age (days)	Class	Intact‡	20–35%	40–80%	85–100%
10	A		4	2	
	B			2§	
18	A	1§			
	B		3	2	1
	C			2	4

N.B. It is apparent that among 10-day-old animals, the (unselected) population includes many that are in relatively rapid decline, and showing stronger intestinal aging phenotypes, compared with the long-lived 18-day-old animals, which enjoyed longer, stronger healthspans than their original colleagues, most of which were long dead. The paucity of 10-day-old animals with healthy intestines speaks to the likelihood that aging in this tissue is a principal influence on healthspan and survival.

†Number of animals scored in that category by TEM measurements.

Measurements in aged animals were compared with the measurements in young adult wild-type animals.

‡Intact category includes animals whose average shortening was 15% or less.

§Includes an animal that showed intestinal nucleus being phagocytosed.

animal's survival, as it reinforces the apical plasma membrane and may prevent the invasion of bacteria into the cytoplasm or the body cavity even if the plasma membrane is breached. As the loss of microvilli has been shown to cause rapid starvation and death (MacQueen *et al.*, 2005), it is likely that the class 'B' and class 'C' animals progressively have nutrient sensing and/or absorption deficiencies. The loss of villi and restriction of a patent lumen, combined with a decreased pharyngeal pumping rate (Collins *et al.*, 2008), all contribute to impaired intestinal function.

Using TEM, we compared the status of microvilli in many thin sections along the length of individual animals and found that their status varied cell by cell within single animals of all behavioral classes (Figs 4 and S2, Table 1). Shortened villi could be found in some cells at any point along the lumen, as far forward as the INT1 cells, and as far posteriorly as the INT9 cells, but the degree of damage to villi differed cell by cell. In some cases, a total loss of villi was noted locally within one intestinal cell or cell pair (Fig. 4). Similar types of changes in microvilli could be found in both 10-day-old and 18-day-old animals (Table 1). In 10-day-old animals, rather severe changes could already be found in class 'B' animals. In 18-day-old animals, class 'C' animals tended to show the more severe changes and the shortest microvilli. Relatively healthy microvilli were sometimes found in regions where the intestine is strongly distorted by the growing germline tissue, suggesting that events on the luminal side of the tissue were independent of stresses on the basal pole. In some locales, individual bacteria were attached firmly to the base of the villi or had seemingly gouged their way into the villi in a manner suggesting that they may be causing local damage (Fig. 4I–N). The bacteria that were capable of corroding the luminal microvilli had a different shape and were much more densely staining than typical bacteria found elsewhere in the lumen. However, very short villi could be found in regions where no bacteria were (still) accumulated (not shown). These villi were often very short, thinner in breadth, and sometimes completely missing (Fig. 4).

Individual cells also showed distinctive variations in cytoplasmic details that help to emphasize the stochastic nature of morphological change. Some cells display concentrations of lipid droplets (Herndon *et al.*, 2002) or huge numbers of seemingly empty vacuoles. Some show an almost lytic cytoplasm with very low electron density, or occasionally, increased cytoplasmic staining (not shown). In rare cases, individual intestinal cells appear to become reduced in cytoplasmic volume compared with their neighbors, suggesting that autophagy may progressively degrade other components besides the nucleus (not shown). Thus, the intestine shows regional variations that may be governed locally, perhaps by cell-specific nuclear changes, or even by the local effects of bacterial attack.

Intestines lose nuclei with age

In mammals, loss of cells with age is a hallmark of a number of tissues including heart and muscle. However, the loss of key cell types or critical nuclei in invertebrate models of aging is much

less well characterized. One of the most striking age-related phenotypes we report here is a dramatic degradation of intestinal nuclei. To describe changes in the intestinal nuclei with age, we carried out DAPI staining of multiple old and young nematodes (Fig. 5). We have previously shown a loss of tail hypodermal nuclei, accumulations of chromatin in the germline of aged *C. elegans* (Golden *et al.*, 2007), and progressive changes in muscle nuclei (Herndon *et al.*, 2002). Others have reported age-related changes in nuclear architecture such as disrupted lamins (Haithcock *et al.*, 2005), but changes in intestinal nuclei have not been described. Of note, the intestinal nuclei are completely fate-mapped in the young adult and are responsible for maintaining intestine function. We report here that these large intestinal nuclei degrade with age (Figs 6 and 7, Movie S4). In very old animals, many intestinal nuclei are undetectable by DAPI staining (Fig. 6A–B, Movie S4) or methylene blue/pararosaniline staining (Figs 6D and S3). By day 12 (day 0 being the day laid), some intestinal nuclei are visibly smaller than 4- or 8-day-old intestinal nuclei (Fig. 6C). Intestinal nuclei continue to degrade with age, and by day 20, many are completely undetectable by DAPI staining or by visualizing stained tissue sections (Figs 6 and S3). The average number of intestinal nuclei decreases from 30 in young 4-day-old wild-type hermaphrodites ($n = 15$ animals,

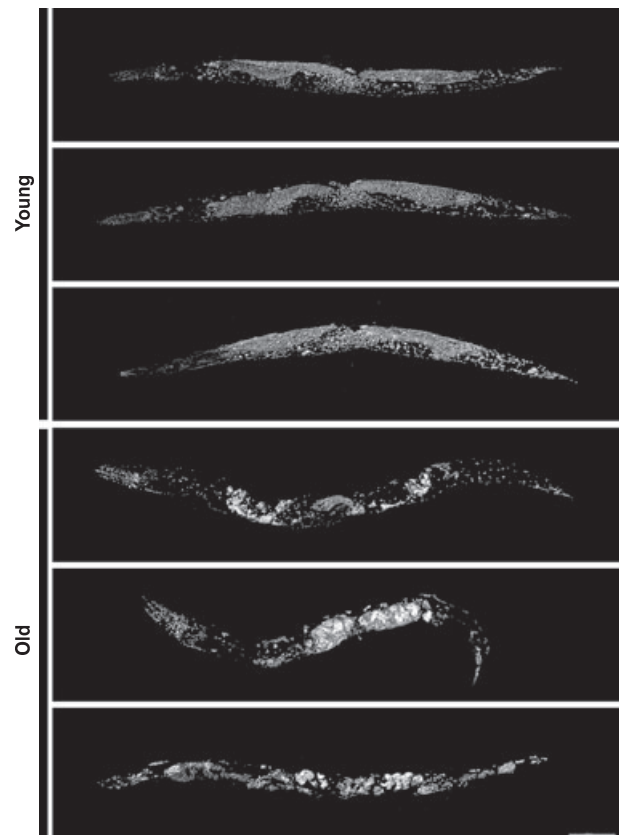


Fig. 5 Nuclear appearance and degradation is hypervariable in old animals. Surface models of DAPI-stained young (4-day-old) and old (20-day-old) wild-type worms. All types of nuclei are subject to variations in old age, including those of the intestine, muscles, germline, and others. Scale bar is 100 μm .

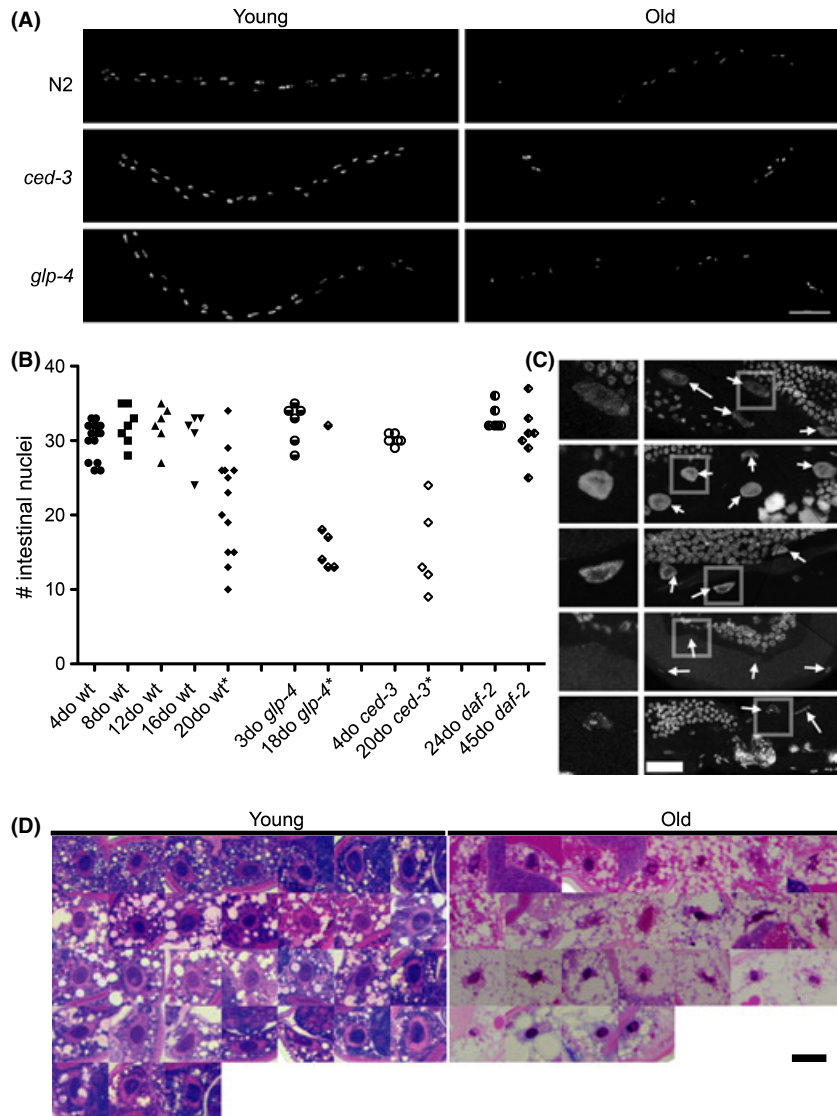


Fig. 6 Aging intestines lose nuclei. (A) Surface model of intestinal nuclei from DAPI staining of a young and old adult wild-type, *ced-3*, or *glp-4* worm. Scale bar is 100 μ m. (B) Graph showing the number of intestinal nuclei in 4, 8, 12, and 20-day-old wild-type, 3 and 18-day-old *glp-4*, 4- and 20-day-old *ced-3*, and 24- and 45-day-old *daf-2* worms. Intestinal nuclei were identified from DAPI staining based on location and morphology. *P* values are calculated based on a one-tail two-sample equal variance *t* test. (**P* < 0.05). (C) Representative intestinal nuclei from a 4, 8, 12, 16, and 20-day-old wild-type worm. Intestinal nuclei are often fainter and smaller (day 16 and 20). Boxed region is enlarged in panel. Arrows indicate intestinal nuclei. (D) All the intestinal nuclei from a young (4-day-old) and old (20-day-old) wild-type worm. Images are from methylene blue/pararosaniline-stained sections. Overall staining of cytoplasm is very different because of the lack of ground substance or typical organelles, and an increase in lipid storage. Scale bar is 10 μ m.

± 0.6 SE) to 22 in old 20-day-old animals ($n = 13$ animals, ± 1.9 SE, $P = 0.001$). The remaining intestinal nuclei were visibly smaller (Fig. 6A,C–D). This degradation and loss of nuclei occurs throughout the intestine, but seems most severe in the anterior half of the worm. Young wild-type worms had between 33 and 26 intestinal nuclei, consistent with the fate map of young *C. elegans*. However, old worms ranged from 34 to as low as 10. This remarkable stochastic loss of nuclei with age represents another example of increased variability with age (Table 2). Although intestinal nuclei have begun to degrade by day 12 (Fig. 6C), there is no significant loss of nuclei in 8-day-old (32 nuclei, $n = 7$ animals, ± 0.3 SE, $P = 0.07$), 12-day-old (32 nuclei, $n = 6$ animals, ± 3.1 SE, $P = 0.08$), or 16-day-old (31 nuclei, $n = 5 \pm 1.7$ SE, $P = 0.4$) wild-type hermaphrodites compared with 4-day-olds (Table 2, Fig. 6B).

Given that we observed a significant loss of intestinal nuclei with age, we hypothesized that such a loss was dependent on apoptotic mechanisms. Although we did not

detect any loss of intestinal cells, we hypothesized that there could be some cellular loss we failed to observe or cells could be only partially undergoing apoptosis and not getting engulfed. Apoptosis is one way age-damaged cells can be prevented from forming tumors, while senescence is another (Campisi, 2005). As the caspase *ced-3* (Ellis & Horvitz, 1986) is required for apoptosis, we wished to establish whether the number of nuclei in a *ced-3* apoptosis-deficient strain is different from the number of nuclei in wild-type animals. Young *ced-3* loss of function mutants had 30 intestinal nuclei ($n = 6$, ± 0.8 SE) compared with 15 nuclei in old (20-day-old) *ced-3* mutants ($n = 5$, ± 2.7 SE, $P = 0.0001$) (Fig. 6). These results therefore demonstrate that the age-related loss of intestinal nuclei is not apoptosis dependent.

To test how the germline might contribute to the loss of intestinal nuclei, we also counted nuclei in *glp-4* worms, which fail to create a germline. We found that aged *glp-4* worms also had significantly fewer intestinal nuclei (18, $n = 6$, ± 3.0) than young

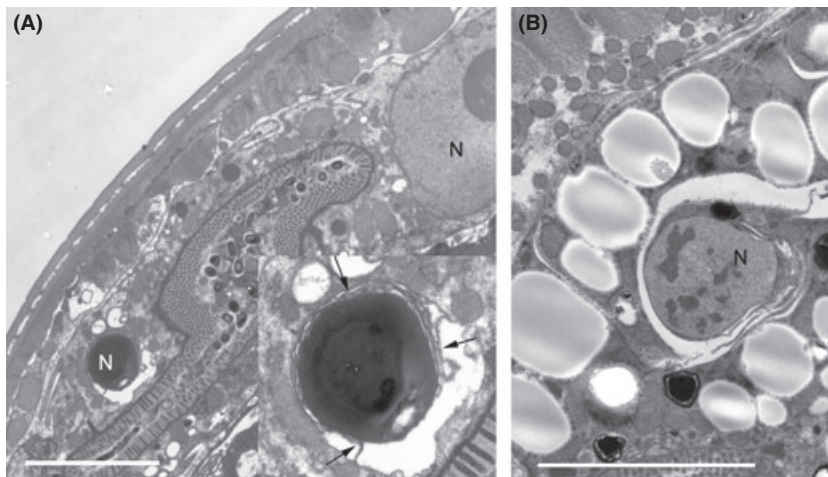


Fig. 7 Nuclear autophagy in old adults. Panel A shows a 10-day-old class 'B' animal in the midbody, where the intestine has been pushed into a thin dorsal wedge by swelling of the uterus. Two intestinal nuclei are seen, a full-sized nucleus on the right and a shrunken dark-staining nucleus undergoing phagocytosis on the left. Arrows (inset in A) indicate internal membranes enveloping the shrunken nucleus. N, nucleus. Panel B shows an 18-day-old class 'A' animal. Here, a single nucleus is seen, reduced in size, and undergoing phagocytosis. Scale bars indicate 0.5 μm .

Table 2 Intestinal nuclei loss

Strain	Median survival	Animals scored (censored)	Age	Survival	Mean intestinal nuclei (n)	t -test P value (compared with youngest)	F test P value (compared with youngest)
N2	20	1241 (697)	4	1.00	30 (15)		
			8	0.99	32 (7)	0.07	0.8
			12	0.85	32 (6)	0.08	0.6
			16	0.59	31 (5)	0.4	0.2
			20	0.40	22 (13)	< 0.0001	0.0005
<i>glp-4</i> (25°)	10	476 (141)	3	1.00	32 (6)		
<i>ced-3</i>	20	399 (222)	4	1.00	30 (6)		
			20	0.39	15 (5)	< 0.0001	0.0003
<i>daf-2</i>	42	390 (271)	24	0.66	33 (6)		
			45	0.20	31 (7)	0.1	0.1

glp-4 intestines (32, $n = 6$, ± 1.1 , $P = 0.0005$). As *glp-4* worms are never under pressure from growth of the reproductive system and the intestinal nuclei are still reduced during aging, we conclude that the age-related degradation of intestinal nuclei is independent of germline development.

We next asked whether the long-lived *daf-2(e1370)* strain has a delayed loss of nuclei and found that it indeed does. Even by day 45, which is well past the maximum lifespan of wild-type worms, there is an average of 31 intestinal nuclei ($n = 7$) (Table 2, Fig. 6B). Intestinal nuclei from 20-day-old *daf-2(e1370)* worms also appear to be somewhat protected from age-related degradation by methylene blue and pararosaniline staining compared with intestinal nuclei from similarly aged wild-type worms (Fig. S3).

Intestinal nuclei appear to gradually degrade (Fig. 6C), but may retain some structure. Methylene blue/pararosaniline-stained intestinal nuclei from old *C. elegans* are smaller and irregular compared with young intestinal nuclei (Fig. 6D). Old nuclei become increasingly difficult to distinguish from background as the germline swells (Golden *et al.*, 2007) and the intestinal nuclei shrink with age (Fig. 6A,C–D), leaving the possibility of some nuclear remnants remaining when they cannot be

resolved by DAPI. We attempted to confirm our data in living worms using an NLS::GFP expressed in the intestine, but found it too variable and difficult to distinguish from the normal gut autofluorescence that increases with age to be a reliable marker (data not shown). Additionally, the increase in autofluorescent lipofuscin (Clokey & Jacobson, 1986; Gerstbrein *et al.*, 2005) made distinguishing intestinal nuclei by a GFP marker in live worms very difficult. In a strain expressing lamin::GFP, lamin was sometimes observed at the periphery of apparent nuclei despite no detectable DAPI staining in 20-day-old worms (data not shown), suggesting that some components of the corpse of the nucleus remain.

At the TEM level, we were not able to make such comprehensive surveys of nuclei as was made with LM serial sections. However, we noted cases at both 10 days and at 18 days where single intestinal nuclei had shrunken, become darker-stained, and appeared to be undergoing autophagy within the intestinal cytoplasm of a class 'A' (at 18 days) or class 'B' (at 10 days) animal (Fig. 7). Such occurrences may not remain visible for very long, so we surmise that this may be a common route by which shrinking nuclei finally disappear from view. Nuclear loss is an ongoing process even in the healthiest old animals and may

precede and precipitate progressive changes in intestinal morphology as transcription becomes impossible.

Discussion

We report here a number of novel, age-related changes in *C. elegans* that arise at the cellular level. These include an increase in the variability of the shape and size of the intestinal lumen, a loss or foreshortening of microvilli in regions of the intestine, and a loss of intestinal nuclei with age. These intestinal changes are likely highly deleterious to the aging worm. As the exact cause of death in aging worms has never been clearly established, it will be interesting to explore to what extent intestinal changes may directly contribute to the death of the nematode or whether they are a secondary effect of another aging phenotype. We report here for the first time that the intestine, a major functional tissue in *C. elegans*, shows a substantial loss with age and that this loss is highly stochastic among individuals and also among intestinal cells within individuals. The loss of nuclei in the intestine of the aging worm is an example of an age-related stochastic event that could have severe deleterious functional changes. Other changes to the intestinal cytoplasm, including accumulations of unusual membrane-bound vesicles, lipid vesicles, and dramatic changes in the density of the ground substance of the cytoplasm were also common and differed from one cell to another along the length of the intestine.

We also observed severe changes in the intestinal lumen including irregular luminal morphology, a degradation and later loss of microvilli, live bacterial accumulation, and 'pinching' of the lumen in regions containing germline swelling (Golden et al., 2007). Feeding *C. elegans* live OP50 *E. coli* is standard laboratory procedure, although feeding worms live *E. coli* is known to cause a shortened lifespan compared with dead bacteria (Garigan et al., 2002), less pathogenic bacteria (Garsin et al., 2003), or growth in bacteria-free media (Szewczyk et al., 2006). Although decreased pathogenicity is likely the cause of these lifespan extensions, it is formally possible that they could be attributed to nutritional changes. Therefore, *E. coli* infection seems one likely cause of microvillar loss or the other changes in intestinal morphology we observed in old individuals, based on the TEM data in particular (Fig. 4). However, we never observed live bacteria entering the cytoplasm of the intestinal cells nor invading the adherens junctions of the intestinal cells.

Changes in microvillar structure seem likely to involve two parallel mechanisms. First, in almost all intestinal cells, microvilli are markedly reduced in length by 10 days of adulthood, even in the absence of any pathogenic bacteria nearby. This reduction seems to be cell-specific, as individual cells show markedly different length changes within the same animal. Secondly, in a few places within an animal, local changes in the intact *E. coli* inside the lumen can produce clusters of smaller, dark-staining pathogenic bacteria that grossly degrade the microvilli even further. These bacteria can insert deeply between villi, perhaps defeating protection by the glycocalyx and leading to local loss of microvilli in patches. In 18-day-old adults, occasional patches

with complete loss of villi were noted where the bacteria were no longer present.

One possibility is that the germline swelling in old animals could either be causing a physical stress to the intestine or errant signaling that results in intestinal changes. However, we found that the *glp-4* mutant, which does not have a developed germline, still had a loss of intestinal nuclei with age. Not surprisingly, the angularity of the intestine was less tortuous than wild-type worms with germline swelling. This suggests that although the germline swelling could still play a role in aging of the intestine, it does not explain all the phenotypes we observed. In particular, in wild-type aged adults, zones with extreme compression of the intestine by a swollen germline could still display relatively healthy microvilli (Fig. 7A). It remains possible that signaling from the somatic gonad may affect age-related changes in the intestinal lumen.

Old worms have a dramatic loss of intestinal nuclei that could severely affect the ability of the intestine to transcribe new mRNA. This begins by day 10, when a few small nuclei already appear to be inside autophagosomes (Fig. 7), and is more pronounced by day 12, when some worms have visibly smaller, but not absent, nuclei when stained with DAPI. Autophagy is a mechanism by which the cell is able to recycle its cytoplasmic contents for many processes (Melendez & Levine, 2009) such as cell maintenance or survival during starvation (Kang et al., 2007). As autophagy has been previously shown to be required for lifespan extension in long-lived *daf-2* (Melendez et al., 2003) or diet-restricted worms (Jia & Levine, 2007), it is possible that the old animals we observe with intestinal nuclei loss are able to survive by recycling their cellular components via autophagy. Previously, we reported a loss of nuclei in the tail with age (Golden et al., 2007). Besides autophagy, one possible explanation for the absence of DAPI staining is that an age-related change in chromatin state results in lower fluorescence of the DNA-binding dye DAPI. Indeed, changes in histone expression with age and changes in histone modification are already known to occur in *C. elegans* with age (Oberdoerffer & Sinclair, 2007; Golden et al., 2008), and a decrease in the DAPI fluorescence of euchromatin compared with heterochromatin has been observed previously (Fujita et al., 1999; Iovene et al., 2008). Visible changes in the chromatin are obvious in some nuclei by 10 days of age in electron micrographs (Fig. 7). Regardless of whether the absence of DAPI staining is because of a loss of DNA or an alteration of the chromatin state of intestinal cells, this would result in an altered transcriptional profile of the intestinal cells. Owing to the confirmation of intestinal nuclei loss and degradation by histological staining of fixed sections we present in this manuscript, it is unlikely that a change in chromatin state is the only explanation for an absence of intestinal nuclei by DAPI staining. An age-related apoptotic process is also unlikely to explain the loss of nuclei, because there was no change in the number of nuclei in aged *ced-3* mutants compared with wild-type, and many intestinal cells appeared intact by electron microscopy. Autophagy remains a more likely mechanism by which some intestinal nuclei are lost.

Although some intestinal cells had no detectable DAPI staining, we occasionally observed a nuclear envelope in lamin::GFP intestinal cells with no DAPI-positive nuclei. This suggests that these nuclei either have a loss of DNA but some remnants of a nucleus remain, that these nuclei are in the midst of autophagy, or that these nuclei just have an altered chromatin state. As it is known that the nuclear envelope degrades with age (Haithcock *et al.*, 2005), it is possible that changes in nuclear envelope proteins are contributing to the loss of nuclei we observe.

In summary, we have developed multiple complementary techniques to describe in detail age-related morphological changes in the nematode *C. elegans*. Our approach affords a unique opportunity to completely describe pathological changes in both wild-type and mutant strains of *C. elegans* by reconstructing the aged nematode in three dimensions. This allows us to gather general data on many tissues and organelles simultaneously and then perform targeted experiments including immunohistochemistry and transmission electron microscopy. In this study, we focused on the changes in the aging intestine. We found that this critical tissue undergoes dramatic changes in structure and contents with age. In particular, we discovered that there are stochastic losses of nuclei and microvilli within individual intestinal cells of aging animals. Using approaches similar to those we describe here, it is clearly possible to explore the pathological changes that occur under different environmental and genetic conditions that influence lifespan. By applying this workflow to other tissues, we may discover other compelling, novel, age-related phenotypes. Many nuclei and cells, such as vulval or hypodermal cells, can be identified based on positioning and morphology, while more tightly packed cells like those in the head will require additional histological or transgenic markers. This can contribute to a better understanding of the pathophysiology of aging in model systems, especially by making use of model systems in which lifespan extension is routinely accomplished by either environmental or genetic manipulations.

Experimental procedures

Nematode strains and culture conditions

Strains used were wild-type Bristol N2, *ced-3(n717) IV*, *glp-4(bn2) I*, *daf-2(e1370)*, *lmn-1::gfp LW0700(ccls4812) X*, and QC82. Nematodes were grown at 20°C on NGM plates spotted with the *E. coli* strain OP50. The *glp-4(bn2) I* strain was grown at the restrictive temperature of 25°C for experiments. Synchronized populations were acquired by allowing adult parents to lay eggs for 2–4 h before removing them (day 0). After reaching sexual maturity, the synchronized nematodes were transferred to fresh plates daily until past reproductive age. LW0700 (Haithcock *et al.*, 2005) was provided by Jun Liu, Cornell University. The remaining nematode strains and *Escherichia coli* strain OP50 used in this work were provided by the *Caenorhabditis* Genetics Center, which is funded by the National Institutes of Health National Center for Research Resources (NCRR).

Tissue sectioning

Worms were embedded in plastic and sectioned at 0.5 μm using an MT-7000 ultramicrotome (RMC Products). Sections were stained with 0.125 mg mL⁻¹ pararosaniline and 0.375 mg mL⁻¹ methylene blue in 23.75% ethanol buffered pH 6.8–7.2. Sections were rinsed in water, dried, and mounted in DPX (modified from Energy Beam Sciences Methylene Blue – Basic Fuchsin, Lee's protocol). Sections were imaged using a 63X objective on a Zeiss Axioplan 2. Images were digitally aligned using custom software based on ITK (Yoo *et al.*, 2002) and manually refined using Photoshop (Adobe Systems Inc., San Jose, CA, USA). Tissue segmentation was performed using Imaris (Bitplane Scientific Software, Zurich, Switzerland) and rendered using Imaris or Cinema 4d (Maxon Computer Inc., Friedrichsdorf, Germany). As histological staining of sectioned tissues is not a common technique in *C. elegans*, structures were identified based on similarities with electron microscopic data (Hall & Altun, 2008) or our confocal data.

Fluorescence imaging

For antibody staining, nematodes were picked into a small drop of water (~5 μL) on a glass coverslip. A small dab of vacuum silicon grease (Beckman) was placed in each corner to avoid squishing the nematodes. Slides were freeze-cracked, fixed in –20°C methanol for 10 min, rehydrated in PBS, blocked in 5% nonfat dry milk in PBS + 0.1% triton, and stained overnight in primary antibody diluted in PBS. Slides were then washed, incubated in secondary antibody diluted in PBS, washed, and mounted in Prolong Gold with DAPI (Invitrogen, Carlsbad, CA, USA) using a coverslip with silicon grease in the corners. Worms stained only with DAPI were washed in S basal, fixed in –20°C acetone, washed in S basal, and mounted in Prolong Gold with DAPI. The MH33 mouse monoclonal antibody was used at a dilution of 1:10. The MH33 monoclonal antibody developed by Robert H Waterson, University of Washington, was obtained from the Developmental Studies Hybridoma Bank developed under the auspices of the NICHD and maintained by The University of Iowa, Department of Biology, Iowa City, IA 52242. Anti-guinea pig IgG Alexa Fluor 488 (Invitrogen) and anti-mouse IgG Alexa Fluor 488 (Invitrogen) were used at a dilution of 1:200. Nematodes were visualized using a Zeiss LSM510 inverted confocal microscope and 63X objective. Z stacks were tiled across the area of the worm and stitched using the Zeiss multitime macro or XuvTools (Emmenlauer *et al.*, 2009). Three-dimensional volume reconstructions and surface models of the tiled images were visualized in Imaris. Surface models were created using both manual and automated methods in Imaris. Rendering was performed using Imaris or Cinema 4D.

Transmission electron microscopy

Adult animals were prepared for electron microscopy as previously described (Hall, 1995; Herndon *et al.*, 2002). Briefly, animals were immersed in buffered aldehydes, cut open to allow

fixative to pass the cuticle, stained with osmium tetroxide and then with en bloc uranyl acetate, and embedded in Epon. Thin sections were collected on slot grids, poststained with uranyl acetate and lead citrate, and viewed on a Philips CM10 electron microscope. Structures were identified based on morphology (Hall & Altun, 2008).

Acknowledgments

This work was supported by Geroscience funds awarded to SM from NIH (ULDE019608 & RL1AG032117), support from the Hillblom foundation, and a generous gift from the Glenn Foundation for Medical Research. MG was supported by a TL1 fellowship from the NIH (AG032116). DHH and LAH were supported by NIH RR 12596. Original TEM work on aging *C. elegans* was supported by grants from NINDS and the National Institute on Aging to Monica Driscoll, whom we thank. We also thank Gloria Stephney, Ken Nguyen, Peter Schmeissner, Kristin Listner, and Angela Jevince for their help in the electron microscopy, Rose Rua for help in scanning the archive of TEM images into digital form, and Adam Orr for help in imaging stained tissue sections.

References

- Campisi J (2005) Aging, tumor suppression and cancer: high wire-act! *Mech. Ageing Dev.* **126**, 51–58.
- Ciche TA, Kim KS, Kaufmann-Daszczuk B, Nguyen KC, Hall DH (2008) Cell Invasion and Matricide during *Photobacterium luminescens* Transmission by *Heterorhabditis bacteriophora* Nematodes. *Appl. Environ. Microbiol.* **74**, 2275–2287.
- Clokey GV, Jacobson LA (1986) The autofluorescent “lipofuscin granules” in the intestinal cells of *Caenorhabditis elegans* are secondary lysosomes. *Mech. Ageing Dev.* **35**, 79–94.
- Collins JJ, Huang C, Hughes S, Kornfeld K (2008) The measurement and analysis of age-related changes in *Caenorhabditis elegans*. *WormBook: the online review of C elegans biology*, 1–21.
- Ellis HM, Horvitz HR (1986) Genetic control of programmed cell death in the nematode *C. elegans*. *Cell* **44**, 817–829.
- Emmenlauer M, Ronneberger O, Ponti A, Schwab P, Griffa A, Filippi A, Nitschke R, Driever W, Burkhardt H (2009) XuvTools: free, fast and reliable stitching of large 3D datasets. *J. Microsc.* **233**, 42–60.
- Fujita N, Takebayashi S, Okumura K, Kudo S, Chiba T, Saya H, Nakao M (1999) Methylation-mediated transcriptional silencing in euchromatin by methyl-CpG binding protein MBD1 isoforms. *Mol. Cell. Biol.* **19**, 6415–6426.
- Garigan D, Hsu A-L, Fraser AG, Kamath RS, Ahringer J, Kenyon C (2002) Genetic analysis of tissue aging in *Caenorhabditis elegans*: a role for heat-shock factor and bacterial proliferation. *Genetics* **161**, 1101–1112.
- Garsin DA, Villanueva JM, Begun J, Kim DH, Sifri CD, Calderwood SB, Ruvkun G, Ausubel FM (2003) Long-lived *C. elegans* daf-2 mutants are resistant to bacterial pathogens. *Science* **300**, 1921.
- Gerstbrein B, Stamatias G, Kollias N, Driscoll M (2005) In vivo spectrofluorimetry reveals endogenous biomarkers that report healthspan and dietary restriction in *Caenorhabditis elegans*. *Aging Cell* **4**, 127–137.
- Golden TR, Beckman KB, Lee AHJ, Dudek N, Hubbard A, Samper E, Melov S (2007) Dramatic age-related changes in nuclear and genome copy number in the nematode *Caenorhabditis elegans*. *Aging Cell* **6**, 179–188.
- Golden TR, Hubbard A, Dando C, Herren MA, Melov S (2008) Age-related behaviors have distinct transcriptional profiles in *Caenorhabditis elegans*. *Aging Cell* **7**, 850–865.
- Gomori G (1950) Aldehyde-fuchsin: a new stain for elastic tissue. *Am. J. Clin. Pathol.* **20**, 665–666.
- Haitchcock E, Dayani Y, Neufeld E, Zahand AJ, Feinstein N, Mattout A, Gruenbaum Y, Liu J (2005) Age-related changes of nuclear architecture in *Caenorhabditis elegans*. *Proc. Natl Acad. Sci. USA* **102**, 16690–16695.
- Hall DH (1995) Electron microscopy and three-dimensional image reconstruction. *Methods Cell Biol.* **48**, 395–436.
- Hall DH, Altun ZF (2008) *C. elegans Atlas*. Cold Spring Harbor, New York: Cold Spring Harbor Laboratory Press.
- Hall DH, Winfrey VP, Blaeuer G, Hoffman LH, Furuta T, Rose KL, Hobert O, Greenstein D (1999) Ultrastructural features of the adult hermaphrodite gonad of *Caenorhabditis elegans*: relations between the germ line and soma. *Dev. Biol.* **212**, 101–123.
- Hedgecock EM, White JG (1985) Polyploid tissues in the nematode *Caenorhabditis elegans*. *Dev. Biol.* **107**, 128–133.
- Herndon LA, Schmeissner PJ, Dudaronek JM, Brown PA, Listner KM, Sakano Y, Paupard MC, Hall DH, Driscoll M (2002) Stochastic and genetic factors influence tissue-specific decline in ageing *C. elegans*. *Nature* **419**, 808–814.
- Hosono R (1978) Age dependent changes in the behavior of *Caenorhabditis elegans* on attraction to *Escherichia coli*. *Exp. Gerontol.* **13**, 31–36.
- Iovene M, Wielgus SM, Simon PW, Buell CR, Jiang J (2008) Chromatin structure and physical mapping of chromosome 6 of potato and comparative analyses with tomato. *Genetics* **180**, 1307–1317.
- Iraoqui JE, Troemel ER, Feinbaum RL, Luhachack LG, Cezairliyan BO, Ausubel FM (2010) Distinct pathogenesis and host responses during infection of *C. elegans* by *P. aeruginosa* and *S. aureus*. *PLoS Pathog.* **6**, e1000982.
- Jia K, Levine B (2007) Autophagy is required for dietary restriction-mediated life span extension in *C. elegans*. *Autophagy* **3**, 597–599.
- Johnson TE (2002) Subfield history: *Caenorhabditis elegans* as a system for analysis of the genetics of aging. *Sci. Aging Knowledge Environ.* **2002**, re4.
- Kang C, You YJ, Avery L (2007) Dual roles of autophagy in the survival of *Caenorhabditis elegans* during starvation. *Genes Dev.* **21**, 2161–2171.
- Kimble J, D. Hirsh (1979) “The postembryonic cell lineages of the hermaphrodite and male gonads in *Caenorhabditis elegans*”. *Dev Biol* **70**, 396–417.
- Kimble J, Sharrock WJ (1983) Tissue-specific synthesis of yolk proteins in *Caenorhabditis elegans*. *Dev. Biol.* **96**, 189–196.
- Leung B, Hermann GJ, Priess JR (1999) Organogenesis of the *Caenorhabditis elegans* intestine. *Dev. Biol.* **216**, 114–134.
- MacQueen AJ, Baggett JJ, Perumov N, Bauer RA, Januszewski T, Schriever L, Waddle JA (2005) ACT-5 is an essential *Caenorhabditis elegans* actin required for intestinal microvilli formation. *Mol. Biol. Cell* **16**, 3247–3259.
- Melendez A, Levine B (2009) Autophagy in *C. elegans*. *WormBook: the online review of C elegans biology*, 1–26.
- Melendez A, Tallozy Z, Seaman M, Eskelinen EL, Hall DH, Levine B (2003) Autophagy genes are essential for dauer development and life-span extension in *C. elegans*. *Science* **301**, 1387–1391.
- Oberdoerffer P, Sinclair DA (2007) The role of nuclear architecture in genomic instability and ageing. *Nat. Rev. Mol. Cell Biol.* **8**, 692–702.

Sulston JE, Horvitz HR (1977) Post-embryonic cell lineages of the nematode, *Caenorhabditis elegans*. *Dev. Biol.* **56**, 110–156.

Szewczyk NJ, Udranszky IA, Kozak E, Sunga J, Kim SK, Jacobson LA, Conley CA (2006) Delayed development and lifespan extension as features of metabolic lifestyle alteration in *C. elegans* under dietary restriction. *J. Exp. Biol.* **209**, 4129–4139.

Thomas DR (2010) Sarcopenia. *Clin. Geriatr. Med.* **26**, 331–346.

Yoo TS, Ackerman MJ, Lorensen WE, Schroeder W, Chalana V, Aylward S, Metaxas D, Whitaker R (2002) Engineering and algorithm design for an image processing Api: a technical report on ITK—the Insight Toolkit. *Stud. Health Technol. Inform.* **85**, 586–592.

Supporting Information

Additional supporting information may be found in the online version of this article:

Fig. S1 Heterogeneity in old worms.

Fig. S2 Wild-type microvilli in young adults.

Fig. S3 Long-lived *daf-2* worms have protected nuclear morphology.

Movie S1 4-day-old wild-type worm. All aligned methylene blue/pararosaniline cross sections from a 4-day-old wild-type worm.

Movie S2 20-day-old wild-type worm. All aligned methylene blue/pararosaniline cross sections from a 20-day-old wild-type worm. Anatomical features of interest are labeled.

Movie S3 The Intestinal lumen changes with age. Segmentation of the intestinal lumen (blue) from aligned methylene blue/pararosaniline cross sections (Movies S1 and S2) from a 4-day-old and 20-day-old wild-type worm. Cuticle is yellow. Small gaps in the intestinal lumen are due to imperfect image alignment from shifted or distorted sections.

Movie S4 Intestinal nuclei are lost with age. Nuclei from a 4-day-old and a 20-day-old wild-type worm. Surface models were created from DAPI staining. Blue nuclei are not annotated, red nuclei are proximal germline masses, yellow nuclei are sperm, and light blue nuclei are intestinal nuclei. Partway through the video, all but the intestinal nuclei ‘fall away’. The 20-day-old intestinal nuclei shift to magenta partway through to allow distinction between the 4-day-old intestinal nuclei.

As a service to our authors and readers, this journal provides supporting information supplied by the authors. Such materials are peer-reviewed and may be re-organized for online delivery, but are not copy-edited or typeset. Technical support issues arising from supporting information (other than missing files) should be addressed to the authors.